Ecotoxicology and Environmental Safety 267 (2023) 115642

Contents lists available at ScienceDirect

Ecotoxicology and Environmental Safety

journal homepage: www.elsevier.com/locate/ecoenv

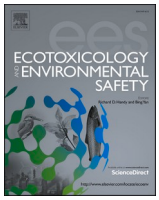

Prioritization of control factors for heavy metals in groundwater based on a source-oriented health risk assessment model

Wenjing Han [a,1], Yujie Pan [b,1], Emily Welsch [b,c], Xiaorui Liu [d], Jiarui Li [b], Shasha Xu [b], Hongxia Peng [e,*], Fangtin Wang [f], Xuan Li [f], Huanhuan Shi [g], Wei Chen [f], Changsheng Huang [f,*]

[a] Geological Survey Research Institute, China University of Geosciences, Wuhan 430074, China
[b] College of Environmental Sciences and Engineering, Peking University, Beijing 100871, China
[c] Department of Geography and Environment, The London School of Economics and Political Science, London, UK
[d] China Electric Power Research Institute, Beijing 100192, China
[e] School of Geography and Information Engineering, China University of Geosciences, Wuhan 430074, China
[f] Wuhan Center of Geological Survey of China Geological Survey, Wuhan 430205, China
[g] School of Environment, China University of Geosciences, Wuhan 430074, China

ARTICLE INFO

Edited by G. Liu

Keywords:
Groundwater
Hydrochemical characteristics
Heavy metals
Source analysis
Health risk

ABSTRACT

Heavy metals (HMs) in groundwater seriously threaten ecological safety and human health. To facilitate the effective management of groundwater contamination, priority control factors of HMs in groundwater need to be categorized. A total of 86 groundwater samples were collected from the Huangpi district of Wuhan city, China, during the dry and wet seasons. To determine priority control factors, a source-oriented health risk assessment model was applied to compare the pollution sources and health risks of seven HMs (Cu, Pb, Zn, Cr, Ni, As, and Fe). The results showed that the groundwater had higher As and Fe contents. The sources of HM pollution during the wet period were mainly industrial and agricultural activities and natural sources. During the dry period, origins were more complex due to the addition of domestic discharges, such as sewage wastewater. Industrial activities (74.10% during the wet period), agricultural activities (53.84% during the dry period), and As were identified as the priority control factors for groundwater HMs. The results provide valuable insights for policymakers to coordinate targeted management of HM pollution in groundwater and reduce the cost of HM pollution mitigation.

1. Introduction

Clean water is a fundamental pillar of food security and human health across the globe; however, a staggering 884 million people worldwide still lack access to safe drinking water (Ravindra, Mor, 2019; Nasrabadi et al., 2015; Adeyemi and Ojekunle, 2021). Groundwater is a vital water resource that plays an important role in supporting the livelihoods of over 2 billion people, especially in arid and semiarid regions (Mahapatra et al., 2020). However, industrialization continues to increase the demand for groundwater. By surpassing its self-purification capacity, groundwater environments are facing heavy contamination. Among contamination sources, heavy metals (HMs) represent a significant challenge to the safety of groundwaters, as even low concentrations can be highly toxic, having irreversible adverse effects on human health (Ravindra, Mor, 2019; Nasrabadi et al., 2015; Adeyemi and Ojekunle, 2021). Certain HMs, such as Cr, Pb, and As, are known to be carcinogenic, posing a significant threat to human health. Excessive intake of Cu, Zn, Ni, and Fe can lead to neurotoxic effects and diseases. Studies have shown that approximately 20% of global cancer cases can be attributed to the consumption of unsuitable groundwater and inadequate sanitation. In 2016, human activities near groundwater sources resulted in 829,000 deaths worldwide (Ma et al., 2023; Shi et al., 2022; Zhai et al., 2022). Given the grave consequences of HM contamination and the immense costs associated with water treatment, it is imperative to distinguish its sources and assess the associated health risks quantitatively. Similarly, it is essential to identify priority factors for controlling metal contamination in groundwater (Ma et al., 2023; Shi et al., 2022; Zhai et al., 2022).

* Corresponding authors.
E-mail addresses: penghx@cug.edu.cn (H. Peng), cshuang@cug.edu.cn (C. Huang).
[1] These authors contributed equally to this work

https://doi.org/10.1016/j.ecoenv.2023.115642
Received 9 August 2023; Received in revised form 23 October 2023; Accepted 26 October 2023
Available online 2 November 2023

Classical methods such as HM contamination index analysis are commonly used to assess the contamination level of HMs in groundwater. However, these methods, including the HM pollution index (HPI), the contamination index (CI), and the HM evaluation index (HEI), have limitations. They require a clear critical limit and do not account for factors such as relative toxicity, relative weight, and reference dose (Chorol, Gupta, 2023). For example, Singh et al. (2017) evaluated groundwater contamination of resources by potentially toxic trace elements near the coal mine site of the Korba coal mine in central India. The level of heavy metal contamination in the groundwater zones of active mining areas was evaluated using pollution evaluation indices (HPI, HEI and CI), but in general, the results evaluated by these indices lacked consistency. Therefore, the multiplicative mean method was used to eliminate the contradictions between indices and reclassify them according to this scale to assess the level of heavy metal contamination in groundwater environments of active mining areas. Singh et al. (2020) argued that these methods lacked the distribution of weights of heavy metals and completely ignored the reasonable errors that may be induced by the different quantities of quality classes. As a result, the range of results can be unnaturally large. To address such limitations, this study introduces a novel assessment approach incorporating the standard weight vector (w_j) obtained through entropy weighting into the HPI equation. By utilizing entropy weighting, the HPI method in this study provides a more comprehensive assessment of HM contents in groundwater, integrating considerations of relative toxicity, relative weight, and reference dose.

Moreover, existing studies have not thoroughly quantified the contributions of different pollution sources, potentially obscuring the establishment of accurate pollution control targets (Jiang et al., 2022). Recently, the principal component score-multiple linear regression (APCS/MLR) method has gained popularity in quantifying the identification of HM sources (Zhang et al., 2020; Shi et al., 2022). APCS/MLR can accurately quantify the contribution (%) of each HM, aiding in identifying key sources (Sun et al., 2022; Lv, 2019). Previous studies on the health risks of HMs in groundwater have predominantly utilized the protocols established by the United States Environmental Protection Agency (USEPA) to assess both carcinogenic and noncarcinogenic risks (Jin et al., 2019; Song et al., 2018; Proshad et al., 2022). These studies often overlook the inherent uncertainties associated with their assessments. Many health risk assessment (HRA) studies have relied on conventional models with settled parameters (Brtnický et al., 2019; Gu et al., 2016; Wang et al., 2016). Nonetheless, such point estimation methods may not accurately identify the most significant risk factors due to uncertainties in concentrations and individual variation, potentially leading to skewed estimations of risk levels (Yang et al., 2019; Huang et al., 2021a). Unlike deterministic models, MCS quantifies uncertainties in risk assessment and identifies the influence of exposure pathways and parameters on risk, making it one of the most valuable techniques in this context (Tong et al., 2018; Yang et al., 2019; Dehghani et al., 2021). Increasingly, MCS is being applied to risk assessments of HMs (Dehghani et al., 2021; Ginsberg, Belleggia, 2017). Furthermore, this method considers the differences in toxicity coefficients among different HMs (Liu, Zhang, 2017; Liu et al., 2018). Therefore, a more comprehensive and probabilistic approach, such as MCS, is vital for accurate risk assessment and management strategies.

According to the 2020 hydrogeological survey in China, the Yangtze River Basin is ranked as the second largest underground water resource, boasting 2421.70 billion cubic meters (J. Huang et al., 2021; C. Huang et al., 2021). Among the regions alongside the basin, Wuhan, situated in the middle reaches of the Yangtze River, stands out with the wettest groundwater resources. However, the northeastern Jianghan Plain, including Wuhan, faces environmental challenges due to high Fe, Mn, and As concentrations in the water-bearing medium and overlying soil layers (He et al., 2016). Urbanization and human activities have further exacerbated the degradation of groundwater quality in Wuhan, particularly in the Huangpi District, where groundwater pollution has become increasingly pronounced. The intensification of agricultural and industrial activities has led to escalating demand for water in the Huangpi District. Hence, the prevalence of machine wells has been steadily rising, compounded by private wells, resulting in the exploitation of approximately $2629.42 \times 104\ m^3/a$ of groundwater in the Huangpi district. This situation risks local ecological stability and residents' health (Wu et al., 2021). To address these issues, it is crucial to quantify the impacts of different pollution sources on health risks. Identifying the priority pollution factors for groundwater pollution control in Huangpi District, Wuhan, will be instrumental in enhancing the effectiveness of HM pollution control efforts (Liu et al., 2018).

Here, we have developed an integrated assessment framework by combining entropy-HPI, APCS/MLR, HRA, and MCS methods to comparatively quantify the health risks associated with various sources of groundwater contamination in Wuhan city, China. The groundwater assessment was conducted over two seasons, one with dry conditions and the other with wet water. The main objectives of the study are to (1) assess the contamination levels of HMs in groundwater, (2) quantify the potential sources of HMs in the groundwater, (3) evaluate the health risks of HMs in the groundwater from different sources of contamination, and (4) prioritize pollution control efforts by analyzing the relationship between contamination levels of HMs and make policy recommendations based on the priority sources and elements of contamination. The findings are significant in allowing decision-makers to determine the priority order of HM pollution control in groundwater. By understanding the health risks associated with different sources of contamination, policymakers can develop targeted and effective strategies to control and reduce groundwater HM pollution.

2. Materials and methods

2.1. Study area

Huangpi District is situated to the north of Wuhan City, Hubei Province, China, with geographical coordinates of 114°09′~114°37′E, 30°40′~31°22′N. It covers an area of 2261 square kilometers. The district experiences a characterized subtropical monsoon climate. The rainfall distribution in the area varies significantly, and the flood season occurs between April and September. The topography of Huangpi District is higher in the north and gradually slopes downward toward the south. The terrain falls within the eastern section of the north bank of the Yangtze River in the Jianghan Plain (Fig. 1a). It is composed of low hills with tectonic denudation in the north, postlike plains with denudation in the middle, and river alluvial plains in the south. The categories of this study are loose rock pore water, clastic rock fracture pore water, metamorphic rock fracture water, magmatic rock fracture water, and carbonate rock fracture karst water (Fig. 1b). Among these categories, metamorphic fracture water has the most expansive distribution area and is primarily stored in the Hong'an Group of the Yuangu boundary. The groundwater in Huangpi is mainly formed through river water infiltration or atmospheric precipitation, with recharge occurring through submerged layer cross-flow. The predominant direction of groundwater flow is from north to south or from northwest to south. Huangpi District has a population of approximately 1.24 million, and most residents are engaged in agricultural activities, with well-developed farming and breeding industries. However, at this stage, most of the domestic sewage in rural areas is discharged directly into the waterways without treatment, resulting in serious nitrogen and phosphorus pollution and pesticide contamination from agricultural production. Huangpi District is the most important agricultural base in Wuhan. In recent years, heavy metal pollution caused by long-term cultivation and rapid urbanization and industrialization has seriously affected the local soil ecosystem in the area (Guo et al., 2017; Yu et al., 2014).

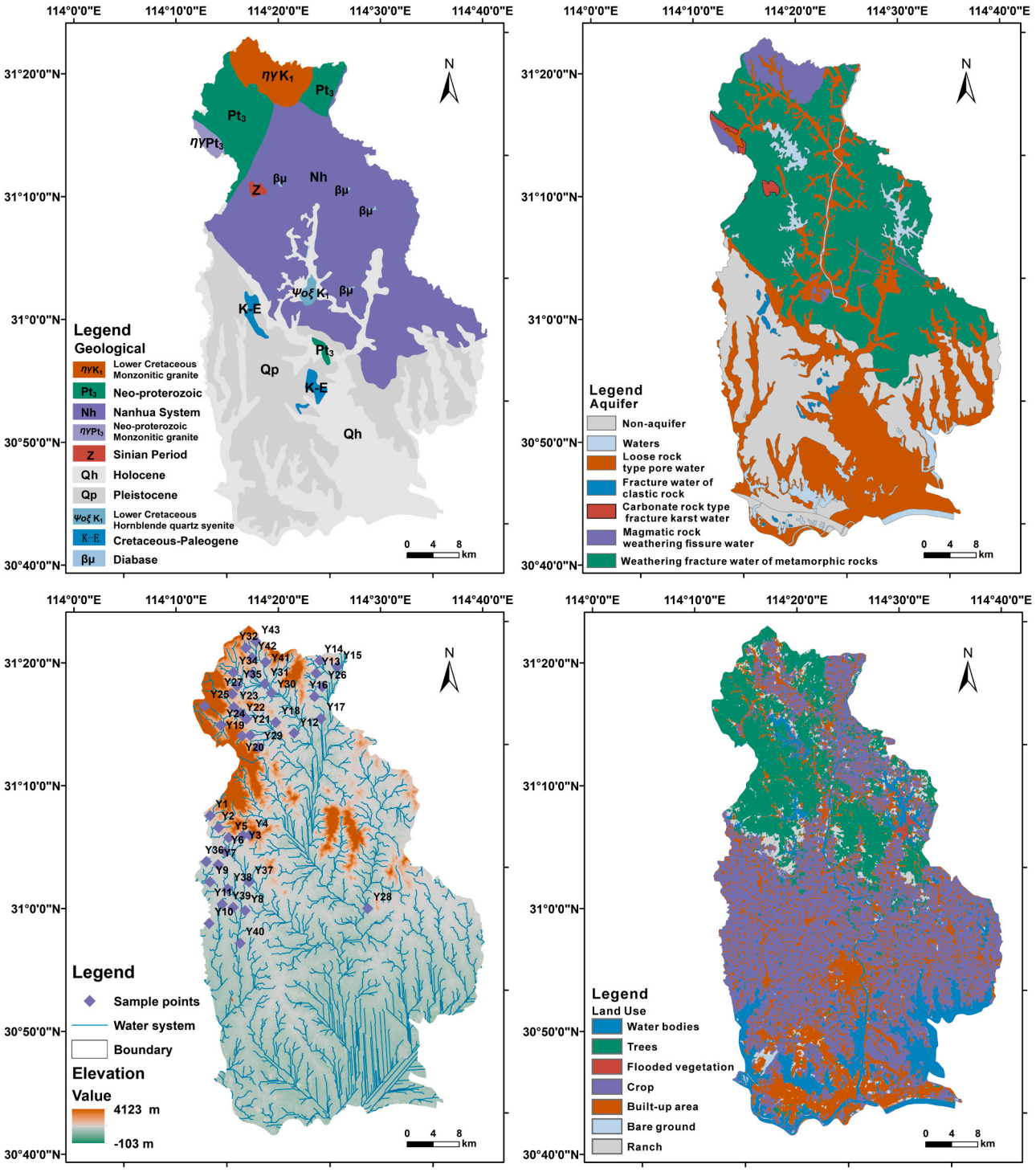

Fig. 1. Overview of the study area: (a) lithological map, (b) hydrogeological map, (c) sampling point map, and (d) land use pattern map.

2.2. Sample collection and analysis

In 2019, 43 groundwater samples were collected during two distinct periods: the water period (July to August) and the dry water period (November to December), for a total of 86 samples collected (Fig. 1c). The sample collection process and quality control measures followed the guidelines outlined in the Regional Groundwater Pollution Investigation and Evaluation Specification (DZ T0288–2015). The field maps used during the investigation were 1:50,000 hydrogeological maps, which can meet the requirements of investigation accuracy. Groundwater samples were collected at irregular densities. Metamorphic fracture water samples were primarily obtained from civil wells with depths of less than 12 m. Civilian wells are often contaminated, with varying degrees of contamination from household to household. Groundwater pollution in the district is mainly found in individual residential villages within the distribution area of pore water of the fourth system and weathered fissure water of metamorphic rocks, such as the civil wells in Changxuanling village.

Groundwater samples were sent to the South Central Mineral Resources Supervision and Testing Center in China for experimentation. Chemical indices for the sample tests were divided into two categories: groundwater-significant anions and cations and HM elements. The

major anions and cations (K^+, Na^+, Ca^{2+}, Mg^{2+}, Cl^-, SO_4^{2-}, HCO_3^-, NO_3^-, pH, TDS) were determined using a plasma emission spectrometer (ICAP-6300), and the anions were analyzed using ion chromatography (ICS-1100) (Subhani et al., 2020). The detection limit for each ion was 0.01 mg/L, and the error in determining anions and cations was generally less than 0.1%. We selected for analysis the heavy metal elements that have large concentrations and health impacts in the region. Concentrations of Cu, Pb, Zn, Cr, Fe and Ni were determined by inductively coupled plasma—mass spectrometry (ICPMS-7700X) (Pan et al., 2021; Muhammad et al., 2018; Muhammad et al., 2019; Muhammad et al., 2020a), and concentrations of As were determined by atomic fluorescence spectrometry (Muhammad et al., 2020b; Muhammad et al., 2021; Muhammad et al., 2022; Muhammad et al., 2023). These heavy metal elements are hazardous to human health. For example, the ingestion of groundwater containing high concentrations of Cr, As, Pb, and Ni can affect the functions of the kidneys, lungs, and other organs, leading to bone, cardiovascular, and cerebrovascular diseases. Moreover, high concentrations of Cu, Fe, Mn, and Zn can be toxic to humans (Pan et al., 2023). The results of blank tests showed that their values were lower than the detection limits, the recoveries of empty spikes were between 95% and 120%, and the overall passing rates of the tests were approximately 98.83%. These quality control measures ensured the reliability and accuracy of the sample test results.

2.3. Methods

2.3.1. Evaluation of pollution levels (PI)

The pollution levels were defined as the degree of HM contamination.

$$PI = \frac{C_i}{S_i} \tag{1}$$

C_i is an element's concentration (μg/L), and S_i is the standard value for groundwater (μg/L). The Class III groundwater quality standard (GBT 14848–2017) was used for S_i. A PI value < 0.7 represents no contamination, 0.7–1 is a warning, 1–2 is low, 2–3 is moderate, and ≥ 3 indicates severe contamination.

Entropy, derived initially from thermodynamics, has found applications in various fields and has been utilized to measure a system's level of chaos or disorder (Gao et al., 2009; Liu et al., 2018). In information theory, entropy is used to quantify the level of uncertainty or confusion of information when assessing the presence of meaningful data. Consequently, entropy values can determine weights in specific contexts (Qiao, 2004).

$$X = \begin{bmatrix} X_{11} & \cdots & X_{1m} \\ \vdots & \ddots & \vdots \\ X_{n1} & \cdots & X_{nm} \end{bmatrix} \tag{2}$$

where X_{ij} is the actual measured value of the HMs at the sampling point;.

The calculation of the matrix X is standardized, and the operation uses standardized equations.

$$\text{Satndardizedtreatment} = \begin{cases} \text{PositiveindicatorsX}_{ij} = \dfrac{x_{ij} - \min\{X_j\}}{\max\{x_j\} - \min\{X_j\}} \\ \text{NegativeindicatorsX}_{ij} = \dfrac{\max\{X_j\} - x_{ij}}{\max\{x_j\} - \min\{X_j\}} \end{cases} \tag{3}$$

The decision matrix is normalized as follows:

$$P_{ij} = \frac{X_{ij}}{\sum_{i=1}^{n} X_{ij}} \tag{4}$$

This study used Eq. 5 to calculate information entropy when $P_{ij} = 0$, so $P_{ij} \ln(P_{ij}) = 0$, $\ln(P_{ij})$ is meaningless.

$$e_j = \frac{(-\sum_{i=1}^{n} P_{ij} \mathrm{In} P_{ij}}{\mathrm{Inn}} \tag{5}$$

where e_j is the entropy of the HM element and n is the number of sampling points.

The entropy value is calculated using Eq. 6.

$$W_{bj} = \frac{(1 - e_j)}{m - \sum_{j=1}^{m} e_j} \tag{6}$$

Table S1 in the Supplementary Material contains the results of the entropy weights. The calculated standard weight vector (w_j) obtained using entropic weights was incorporated into the ordinary HPI equation (Eq. 7) to determine the HPI. HPI represents the overall water quality of HMs (Herath et al., 2022; Mohan et al., 1996). The values of HPI range from 0 to 1 and are inversely proportional to the standard allowable values (Si) of the corresponding parameters (Horton, 1965; Mohan et al., 1996). The HPI is calculated using Eq. (7), which incorporates the entropy weights (w_j) obtained from the analysis. This index allows for assessing the water quality concerning HMs and comprehensively evaluating the pollution levels in the studied area.

$$HPI = \frac{\sum_{i=1}^{n} W_i Q_i}{\sum_{i=1}^{n} W_i} \tag{7}$$

where Q_i =subindex for the ith parameter, = unit weight for the ith parameter, and n = number of HMs. According to the HPI values, HM pollution was classified into three categories: low pollution index (<19), medium pollution index (19−38), and high pollution index (>38) (Herath et al., 2022; Chorol, Gupta, 2023).

2.3.2. Absolute principal component scores/multiple linear regression (APCS/MLR) receptor model

The APCS/MLR model is developed from traditional principal component analysis (PCA) and is commonly used to identify HM sources in various environmental media. This model can help decision-makers prioritize pollution treatment strategies. This study utilized the APCS/MLR model by first converting the top factor scores from factor analysis to APCS after standardizing the raw data. Multiple linear regression was then performed on all APCS for each HM content to calculate the contributing factor scores (%) for each HM from different sources (Ma et al., 2018).

Eq. 8 was used for the multiple linear regression calculation (Y. Zhang et al., 2021; W.H. Zhang et al., 2021), where the source contribution values can be negative in APCS/MLR. It is important to note that although these negative contributions are accurate, they may have an impact on the accuracy of the source assignment calculation. Overall, the APCS/MLR model is a valuable tool for identifying and quantifying environmental HM sources, aiding in effective pollution control and resource management. However, negative contribution values in the model highlight the need for careful interpretation and consideration when analyzing the results for source assignment.

$$C_n = \xi_0 + \sum_{k-1}^{p} \xi_k \times \mathrm{APCS}_k \tag{8}$$

where C_n is the concentration, ξ_0 is the intercept of the regression, ξ_k is the regression coefficient, $APCS_k$ is the absolute principal component score of source factor p, and $\xi_k \times APCS_k$ is the average contribution of source p to C_n. To solve this problem, an absolute function was applied to the mean value (of $\xi_k \times APCS_k$) before calculating the percentage contributions of the source (p).

2.3.3. Health risk apportionment (HRA) model

This study utilized the HRA model used by the US Environmental

Protection Agency (USEPA) to evaluate human health risks via ingestion and dermal contact exposure routes in different populations, including adult males, adult females, and children. Adults were categorized as the general population, while children were labeled as the sensitive group due to increased vulnerability. The HMs tested in this study were classified as noncarcinogenic (Cu, Zn, Ni, and Fe) and carcinogenic (Pb, Cr, and As) elements based on findings from previous studies (Shil and Singh, 2019; Panda et al., 2021; Zhou et al., 2019). Human health risks were assessed for both noncarcinogenic and carcinogenic hazards. The noncarcinogenic risk characterization equation (HI) for the exposure model of ingestion and dermal exposure to a specific HM element in groundwater is as follows (USEPA 2011):

$$ADD_{ingestion} = \frac{C \times IR \times EF \times ED}{BW \times AT} \quad (9)$$

$$\mathrm{ADD_{dermal}} = \frac{\mathrm{C \times SA \times PC \times ET \times EF \times ED \times CF}}{\mathrm{BW \times AT}} \quad (10)$$

$$\mathrm{HQ} = \frac{ADD}{\mathrm{RfD}} \quad (11)$$

$$\mathrm{HI} = \sum \mathrm{HQ} \quad (12)$$

ADDingestion and ADDdermal refer to the average daily exposure doses obtained through ingestion and dermal contact. HI > 1 indicates a noncarcinogenic severe risk to human health, while HI < 1 is considered safe.

The equations for the carcinogenic risk (TCR) due to ingestion and dermal exposure are as follows:

$$\mathrm{ILCR} = \frac{\mathrm{ADD \times SF}}{\mathrm{L}} \quad (\mathrm{R} \le 0.01) \quad (13)$$

$$\mathrm{ILCR} = \frac{1 - \exp(-\mathrm{ADD \times SF})}{\mathrm{L}} \quad (\mathrm{R} > 0.01) \quad (14)$$

$$\mathrm{TCR} = \sum \mathrm{ILCR} \quad (15)$$

For TCR $> 1 \times 10^{-4}$ values, the carcinogenic risk is considered intolerable, while TCR $< 10^{-6}$ values indicate a negligible carcinogenic risk to humans (Panda et al., 2021; Guo et al., 2023). Other parameters used to calculate the health risk assessment are shown in Tables S2 and S3.

2.3.4. Monte Carlo simulation (MCS)

This study employed the Monte Carlo approach to simulate the uncertainty of health risks associated with seven HMs (refer to Tables S2 and S3 for the parameters used). MCS is a widely used probabilistic and statistical mathematical theory applied to uncertainty analyses in risk assessment. By utilizing the Monte Carlo simulation method, this study aimed to minimize uncertainty and provide a more robust assessment of carcinogenic and noncarcinogenic health hazards for the populations at each sample site (Karami et al., 2019). In the context of HM health risk assessment, three main factors contribute to uncertainty analysis: exposure parameters, HM concentrations, and the health risk assessment model (Jiang et al., 2021). The study utilized Oracle Crystal Ball to address this uncertainty, conducting 10,000 random simulation iterations to perform the uncertainty analysis. The confidence level was 95% to obtain an approximate solution for the risk assessment. However, the MCS model also has some limitations. For example, it relies on assumed distributions to generate random numbers, which may negatively affect the accuracy of the assessment results. On the other hand, the variability of human exposure parameters may lead to significant differences in the health risks of different populations, and Monte Carlo simulation usually fails to reduce the variability of exposure parameters, which needs to be further optimized by two-dimensional Monte Carlo simulation (2-D MCS) for specific populations in different regions, which can effectively correct the errors of the 1-D MCS by simulating the variables in and out of the loop and overcome the limitation of insufficient exposure parameters among individuals in actual risk assessment to improve the accuracy of risk assessment.

2.3.5. Source-oriented health risk assessment model

The APCS/MLR-HRA model combines the APCS/MLR model and the HRA model to quantitatively assess the human health risk from different allocated sources of HMs (Y. Zhang et al., 2021; W.H. Zhang et al., 2021; R.J. Huang et al., 2018; J. Huang et al., 2018; J. Huang et al., 2021; C. Huang et al., 2021; Ma et al., 2018). The CR of acceptable daily intake (ADD) and HMs I in groundwater sample k can be calculated using Eqs to estimate the CR and NCR (16)-(21):

$$\mathrm{ADD}^k_{ij,ingestion} = \frac{C^k_{ij} \times \mathrm{IR} \times \mathrm{EF} \times \mathrm{ED}}{\mathrm{BW \times AT}} \quad (16)$$

$$\mathrm{ADD}^k_{ij,dermal} = \frac{C^k_{ij} \times \mathrm{SA \times PC \times EF \times ET \times ED \times CF}}{\mathrm{BW \times AT}} \quad (17)$$

$$\mathrm{ILCR}^k_{ij} = \frac{\mathrm{ADD}^k_{ij} \times \mathrm{SF}}{\mathrm{L}} \quad (\mathrm{R} \le 0.01) \quad (18)$$

$$\mathrm{TCR} = \sum \mathrm{ILCR}^k_{ij} \quad (19)$$

$$\mathrm{HQ}^k_{ij} = \sum \frac{\mathrm{ADD}^k_{ij}}{\mathrm{RfD_{ij}}} \quad (20)$$

$$\mathrm{HI} = \sum \mathrm{HQ}^k_{ij} \quad (21)$$

C^k_{ij} is the mass contribution (μg/L) of HM i from source k in sample j (C^k_{ij} is the product of the calculated contribution of source k and its concentration in sample j for the pair). crk ij is the CR of element i in the groundwater sample from source k in groundwater sample j. Eq HQ^k_{ij} is the hazard quotient of HM i in groundwater sample j. The corresponding parameters are Eqs. (9)-(10).

2.4. Statistical analysis

In this study, we used Excel 2016 and SPSS 24.0 for mathematical statistics, Origin 2021 to draw Piper's trilinear map, R language to explore the sources of heavy metal substances and ArcGIS 10.7 to draw hydrogeological sketch maps and location maps of the study area. The probabilistic health risk assessment was carried out using Crystal Ball 11.1.24 software.

3. Results and discussion

3.1. Analysis of pollution characteristics of the groundwater environment

3.1.1. Groundwater chemical characteristics

Table S5 presents the groundwater pH and total dissolved solids (TDS) in the study area during both the wet and dry periods. During the wet period, the pH of groundwater ranged from 3.83 to 7.87, with a mean value of 7.20. The TDS content varied between 142.00 and 1220.00 mg/L, indicating freshwater to slightly saline water. In contrast, during the dry water period, the pH ranged from 6.85 to 8.07, and the TDS content was between 114.00 and 883.00 mg/L. The average concentrations of anions in the study area during both periods were $HCO_3^- > Cl^- > SO_4^{2-} > NO_3^-$, with HCO_3^- predominant. For cations, the mass concentration followed the order $Ca^{2+} > Na^+ > Mg^{2+} > K^+$. The Piper trilinear plot in Fig. 2a demonstrates that the groundwater chemistry in the study area is relatively diverse during the wet period. Cations are mainly distributed in the Ca^{2+}, Na^+ and K^+ terminal elements, while anions are mostly dominated by HCO_3^-. Similar findings were reported by Zhang et al. (2021), who also identified the dissolution

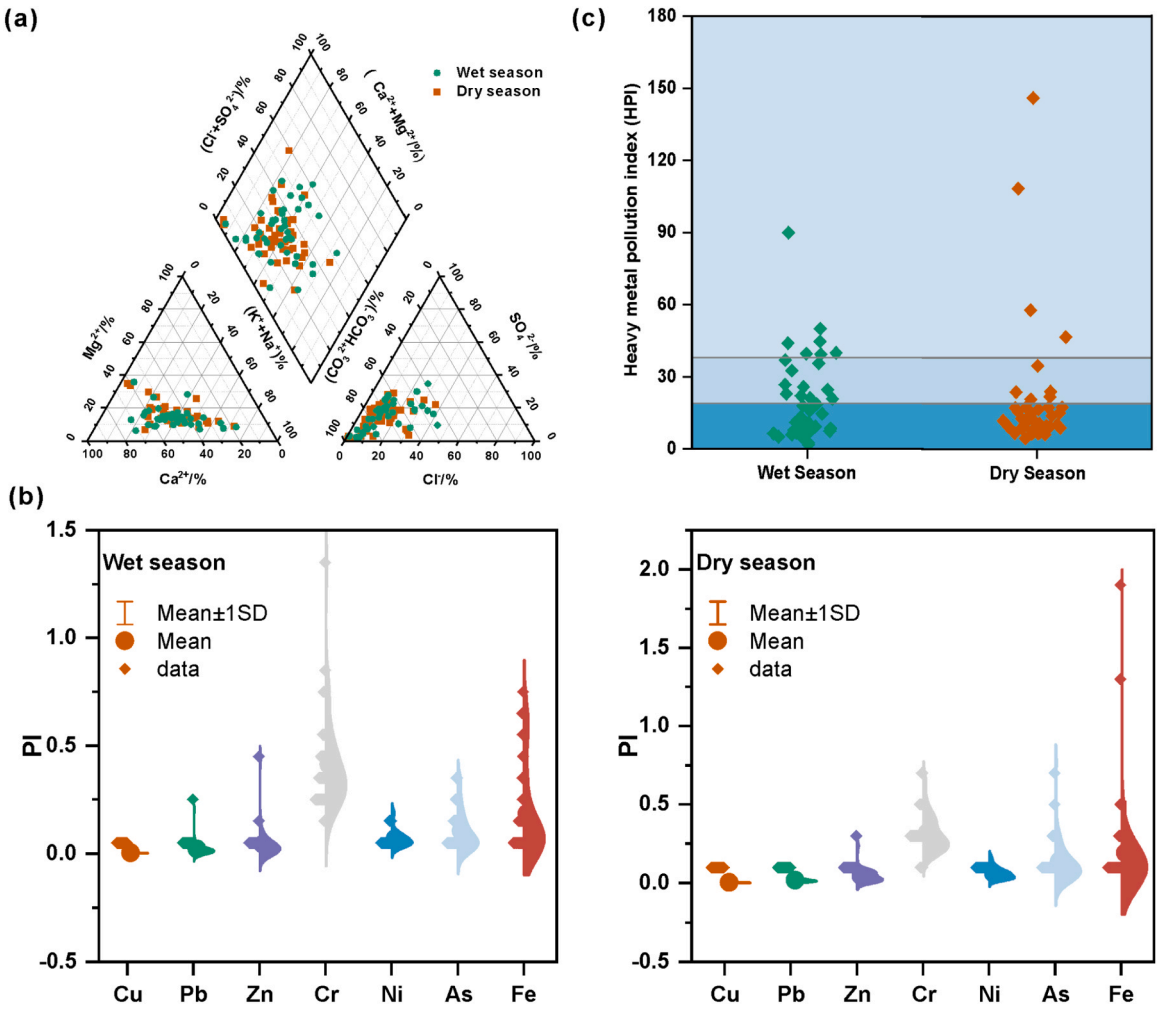

Fig. 2. Groundwater pollution characteristics: (a) piper trilinear map of groundwater chemical characteristics, (b) single factor pollution evaluation, (c) entropy weight-HPI pollution evaluation.

of carbonate rocks as the primary ion source for groundwater in Wuhan. Based on the Shukarev groundwater chemistry type classification, the dominant groundwater chemistry types during the wet period were HCO_3-Na·Ca, HCO_3-Ca, and HCO_3·Cl-Na·Ca. On the other hand, during the dry water period, the dominant types were HCO_3-Na·Ca, HCO_3--Ca·Mg, and HCO_3·Cl-Na·Ca.

3.1.2. *Descriptive statistical analysis*

The results show that Pb, Cr, and Ni during the wet period are higher than those during the dry water period, whereas the averages of Cu, Zn, As, and Fe are lower than those during the dry water period. During the period of abundance, the averages of Cu, Pb, Cr, Zn, Ni, As, and Fe in groundwater were 2.32, 0.20, 42.75, 2.06, 1.39, 1.05, and 55.26 μg/L, respectively, which are all below the limits of the national groundwater quality standard for Class III (GB/T 14848–2017). This is consistent with the results of Li et al., who analyzed the concentrations of the heavy metals Pb, Cd, and As in the direct drinking water of primary and secondary schools in Huangpi District, Wuhan. They concluded that the average mass volume concentrations of heavy metals in the drinking water in this area complied with the Chinese Water Quality Standards for Drinking Water Purification. The coefficient of variation (CV) indicates the overall degree of variability. The CV values for Cu, Pb, Cr, Zn, Ni, As, and Fe were 69.22%, 157.46%, 162.71%, 51.62%, 57.86%, 86.69%, and 112.52%, respectively. This indicates that Cu, Zn, Ni, and As have moderate variability, whereas Pb, Cr, and Fe have high variability. On the other hand, during the dry water period, the average concentrations of Cu, Pb, Cr, Zn, Ni, As, and Fe in groundwater were 3.00, 0.18, 45.44, 1.59, 1.24, 1.37, and 57.43 μg/L, respectively (Table 1). Except for sampling points Y33 and Y41, where the maximum value of element Fe was higher than the national standard for Class III during the dry season, the maximum value of the element at all other sampling points was lower than the national standard for Class III water. Excessive intake of Fe can lead to neurotoxic diseases and even cause various types of cancer. Studies have shown that approximately 20% of global cancer cases can be attributed to the consumption of unsuitable groundwater (Pan et al., 2023). The CV values for Cu, Pb, Cr, Zn, Ni, As, and Fe were 186.54%, 76.51%, 89.65%, 37.55%, 59.53%, 101.08%, and 169.41%, respectively. This indicates that Pb, Cr, Zn, and Ni have moderate variability, while Cu, As, and Fe have high variability. Elemental As in the study area was much higher than in other parts of the basin, while elemental Pb and Fe were lower compared to Shenbei New District. Essential Zn was found in higher concentrations than Cu, Pb, Ni, and As but lower than the groundwater content in Yongqing County (Feng et al., 2016; Liu et al., 2023).

3.1.3. *Groundwater HM pollution levels*

The HPI analysis results (Fig. 2c) showed that the HPI values ranged from 1.80 to 90 during the wet period, with a mean value of 19.73. Approximately 16.28% of the samples were highly contaminated, approximately 23.26% were moderately contaminated, and the remaining samples belonged to the low contamination category. During the dry period, the HPI values ranged from 4.48 to 145.85, with a mean

Table 1
Statistics of HM concentrations (ug/L) in groundwater of Huangpi.

Season	Value	Cu	Pb	Zn	Cr	Ni	As	Fe
Wet season(n = 43)	Mean	2.32	0.20	42.75	2.06	1.39	1.05	55.26
	Min	0.50	0.02	0.61	0.72	0.50	0.10	5.00
	Media	1.71	0.11	24.80	1.75	1.17	0.69	30.40
	Max	8.35	2.03	441.00	6.67	3.89	3.44	212.00
	SD	1.61	0.32	69.55	1.06	0.80	0.91	62.18
	CV%	69.22	157.46	162.71	51.62	57.86	86.69	112.52
Dry season(n = 43)	Mean	3.00	0.18	45.44	1.59	1.24	1.37	57.43
	Min	0.42	0.03	4.12	0.84	0.36	0.18	9.24
	Media	1.44	0.14	34.20	1.38	1.15	1.03	29.70
	Max	30.30	0.80	236.00	3.25	3.43	7.64	552.00
	SD	5.60	0.14	40.74	0.60	0.74	1.39	97.29
	CV%	186.54	76.51	89.65	37.55	59.53	101.08	169.41
Guide value	National standard (grade III)	1000	100	1000	50	20	10	300

value of 20.05; approximately 9.30% of the samples were highly contaminated, approximately 11.63% were moderately contaminated, and the rest belonged to the low contamination category. Based on the above findings, it can be inferred that the pollution level in the study area is higher during dry periods than during wet periods.

3.1.4. Spatial distribution characteristics

From Fig. S1, the high-value areas of Cu and Zn in the two seasons are mainly distributed in the northwestern part of the study area, and the high-value areas of Cr in the two seasons are mainly distributed in the western part of the study area. The pollution level of Pb and As elements in the northern part of the study area in the abundant water period is smaller than that in the dry water period, the pollution level of Ni elements in the abundant water period is higher than that in the dry water period, and the pollution level of Fe elements in the western part of the study area in the abundant water period is much larger than that in the dry water period. In the western part of the study area, the pollution level of Fe is much higher than that in the dry water period.

3.2. Source apportionment of HMs

The correlation between different HMs was assessed using Pearson correlation analysis, after which principal component analysis was employed to determine the major pollution sources. Additionally, the contribution of each pollution source to individual HMs in groundwater was calculated using APCS/MLR. The results of the Kaiser—Meyer—Olkin (KMO) test and Bartlett's test ($P < 0.001$) were consistent with the outcomes of the principal component analysis, confirming the validity of the approach. The fit coefficients (R^2) between the measured concentrations during the wet period and the dry water period ranged from 0.35 to 0.83 and 0.57–0.80, respectively. The ratio of measured concentrations was close to 1, indicating high accuracy and credibility in the constructed APCS/MLR model and its calculated results. During the wet period, three pollution sources were identified by the APCS/MLR model, contributing to Factor I (26.79%), Factor II (50.68%), and Factor III (22.53%) (Fig. 3a). However, the pollution sources during the dry water period were more complex, revealing Factor I (14.52%), Factor II (25.38%), Factor III (34.91%), and Factor IV (25.19%) (Fig. 3b).

During the wet period, the dominant elements in Factor I were Cu (83.43%) and Zn (69.01%) (Figs. 3a-3c). Previous studies have indicated that the continuous application of chemical fertilizers and pesticides in agricultural fields can lead to the accumulation of Cu and Zn (Liu et al., 2018; Yang et al., 2017; Qu et al., 2021). Additionally, herbicides and pesticides employed in agricultural activities contain significant amounts of Cu (Li et al., 2022). According to the local government yearbook report, in 2018 and 2019, the study area was subject to more than 650 tons of pesticides and over 30,000 tons of fertilizers (WHBS, 2018; WHBS, 2019). Animal husbandry, which is vital for local agricultural development in Huangpi District, also contributes to increased Cu and Zn contents due to animal excretions. Based on the current land use situation and the distribution of HMs in the study area (Fig. S1), we observed that high Cu and Zn content values were found in cultivated land. Hence, Factor I can be attributed to agricultural activities. Factor II was dominated by Pb (80.51%), As (91.89%), and Fe (94.75%), which are commonly associated with fossil fuels and wastes from fossil fuel-heavy industries such as metal smelting (Zhai et al., 2022). These elements are introduced into surface water through atmospheric deposition, later infiltrating groundwater aquifers (Ma et al., 2023). A study by Wu et al. (2020) on soil HM pollution sources in Huangpi revealed that the content of Pb is influenced by proximity to industrial enterprises, indicating that industrial pollution is the primary source of Pb. Moreover, areas with high As content are situated near industrial parks in the study area, particularly around electronics factories, metal processing industries, and construction sites. The regions with elevated Fe content are mainly in urban residential areas, potentially affected by domestic wastewater and industrial discharges. According to the local yearbook, Huangpi District had 351 industrial enterprises above a specific scale and nine enterprises with an output value of over 1 billion yuan by the end of 2020 (WHBS, 2020). Therefore, Factor II reflects the influence of industrial activities. Factor III exhibited higher factor loading values for Ni (80.64%) and Cr (49.17%). Table 1 indicates that the coefficients of variation for Ni and Cr are small, suggesting a lesser impact from human activities on these two elements. Previous studies have shown that Cr is primarily controlled by the geological background environment (Dong et al., 2019). Fig. 1 in the appendix illustrates the high Cr content primarily found in open rock-like pore water. As a result of the substantial Cr content in the sediments of the study area, Cr continuously dissolves into the groundwater through leaching, leading to elevated Cr levels in specific areas of the study area. Factor III can be attributed to natural sources.

During the dry period, the sources of HMs become more complex compared to the wet period due to the addition of other domestic sources (Fig. 3d-e). The Factor with the largest variance contribution is Factor III, accounting for 34.91%, making it the primary source of HMs during the dry period. Groundwater factor I in the dry period is mainly influenced by Fe (37.86%), which shows seasonal variations of −104.00 μg/L and −355.50 μg/L at points Y41 and Y42, respectively. These points are in urban residential areas, suggesting a potential influence of human domestic sewage discharge. Therefore, Factor I can be attributed to domestic sources. Factor II is predominantly influenced by As (63.36%), with higher concentrations observed during the dry period compared to the wet period. At point Y33, which has a high concentration of As, there is also an elevated NO_3^- content, primarily associated with human domestic sewage discharge and agricultural activities (Peng et al., 2021). Additionally, the use of As-containing chemicals such as fertilizers and pesticides in agricultural processes, which dissolve directly into the soil and leach into groundwater, can also lead to elevated As levels (Ma et al., 2023). Hence, Factor II is likely related to agricultural sources. Factor III exhibits high factor loading values for Ni

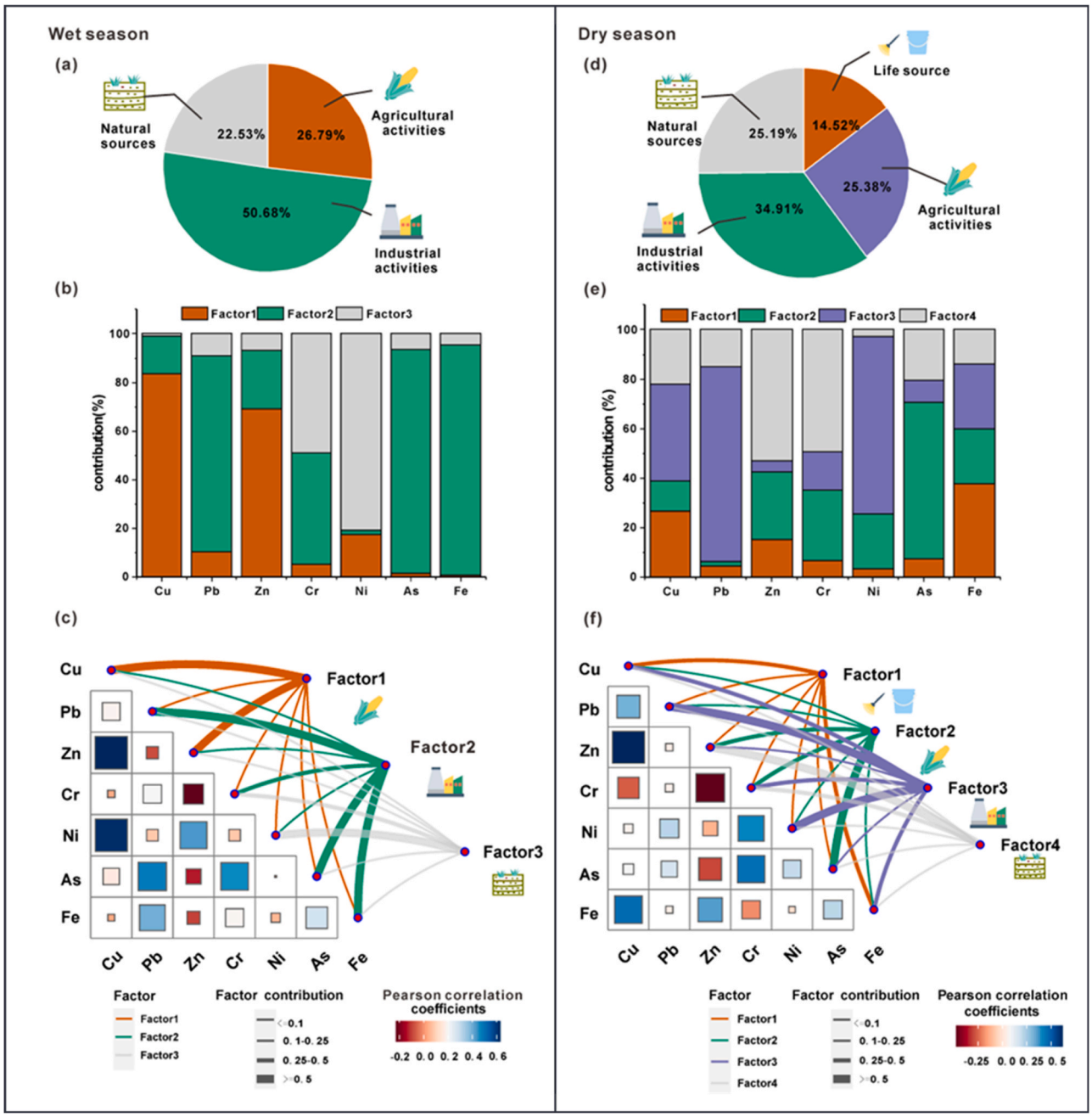

Fig. 3. Analysis of HM sources in groundwater. (a-c) Analysis of HM sources in groundwater during the wet season. (d-f) Analysis of groundwater HM sources in the dry season.

(78.59%) and Pb (71.78%). Ni is an important industrial raw material, and the distribution of Ni in the area is consistent with the presence of electroplating and metal smelting industries, indicating industrial activity as the main source for Factor III. Previous studies have also shown that the amount of Pb in the study area depends on the proximity to the nearest industrial enterprise (Wu et al., 2020), further supporting the notion that industrial activities influence Factor III. Factor IV is dominated by Zn (53.15%) and Cr (49.36%). The coefficients of variation for Cr and Zn are lower than those observed during the wet period, suggesting a minor contribution from external sources. Cr is prevalent in soil parent material and generation processes (J. Huang et al., 2021; C. Huang et al., 2021; Sun et al., 2022). Factor IV is associated with natural sources.

The sources of pollution differ between wet and dry seasons. Some studies have shown that precipitation has some effect on heavy metal concentrations in groundwater. Vaze et al. (2002) concluded that heavy metal concentrations in road runoff are particularly high when short, intense summer storms occur after a long dry period and pollutants accumulate on the road surface. There is a lag between precipitation and shallow groundwater recharge due to surface interception, evaporation from vegetation, and geostratigraphic effects. The concentration content of Cu, Pb, Zn, and Ni in sample site Y20, which is located on both sides of the roadway with nearby automobile repair stores, is much greater during dry periods than during abundant water. Industrial activities and transportation have resulted in elevated concentrations of heavy metals on the road near the sample site. The effects of evaporation and mineral weathering may contribute to the presence of As in groundwater systems, especially during the dry season (Masuda, 2018; Smedley and Kinniburgh, 2002). In addition, cations and heavy metals immobilized on clay minerals may be released into aquifer sediments under microbial

natural evaporation conditions (Nimick et al., 1998; Rasool et al., 2016; Welch et al., 2000). As seen from Table 1, the average value of As in the groundwater during the dry season is greater than that during the abundant season, and the high value of elemental As during the dry season is located at point Y33, which also has a higher concentration of NO_3^- content, which is mainly related to human domestic sewage discharge and agricultural activities. Nilkarnjanakul et al. (2022) also found that the average concentration of As in Quaternary aquifers is greater in the dry season than in the rainy season, and the average concentration of As was less in the dry season than in the wet season. Previous studies have shown that Cr and Ni are mainly controlled by the geological background environment (Dong et al., 2019). The contents of Cr and Ni in groundwater were higher in the abundant water period than in the dry water period. Another explanation is that more heavy metals and trace elements may be leached during the rainy season because the groundwater table is generally higher during the rainy season. In addition, during the rainy season, more chemicals may be washed away directly from the evaporation zone by infiltrating rainwater (Leung and Jiao, 2006).

3.3. Human health risk assessment

3.3.1. Concentration-oriented health risk assessment

The probability distributions of both noncarcinogenic risk (HI) and carcinogenic risk (TCR) for different populations (children, females, and males) during the groundwater abundance and depletion periods were obtained using an MCS (Fig. 4). The mean HI and TCR during the wet period were smaller than those during the dry water period. During the wet period, the mean hazard quotient (HQ) values for all groups were found in the following order: As > Cr > Fe > Pb > Zn > Ni > Cu. On the other hand, during the dry water period, the mean HQ values were found in the following order: As > Cr > Fe > Zn > Pb > Cu > Ni (Table S7). This indicates that the noncarcinogenic risks of As and Cr were higher than those of other heavy elements, and the TCRs for children and adult females were greater than those for adult males. This observation might be attributed to children having lower body weight, leading to relatively higher average daily exposure doses and increased sensitivity to the external environment (Shi et al., 2022). Previous studies have also highlighted that children are more susceptible to HI than adults (Varol, 2019; Varol, Tokatlı, 2022). Sun et al. (J. Huang et al., 2021; C. Huang et al., 2021; Sun et al., 2023) reported that the mean TCR values follow the order of children > adult females > adult males, possibly due to their lower body weight. Consequently, health risk assessments should focus more on children. In both the wet and dry water periods, children exhibited more severe noncarcinogenic risks than adult females and adult males, with the mean HI values following the order: children > adult females > adult males. Previous studies have suggested that when the HQ value is at a 95% probability and remains below the acceptable risk threshold (HQ=1), the health risk associated with HMs in groundwater can be considered below an acceptable level (Yuan et al., 2023). According to the probability distribution analysis, the HI values for all three populations were below the threshold of 1

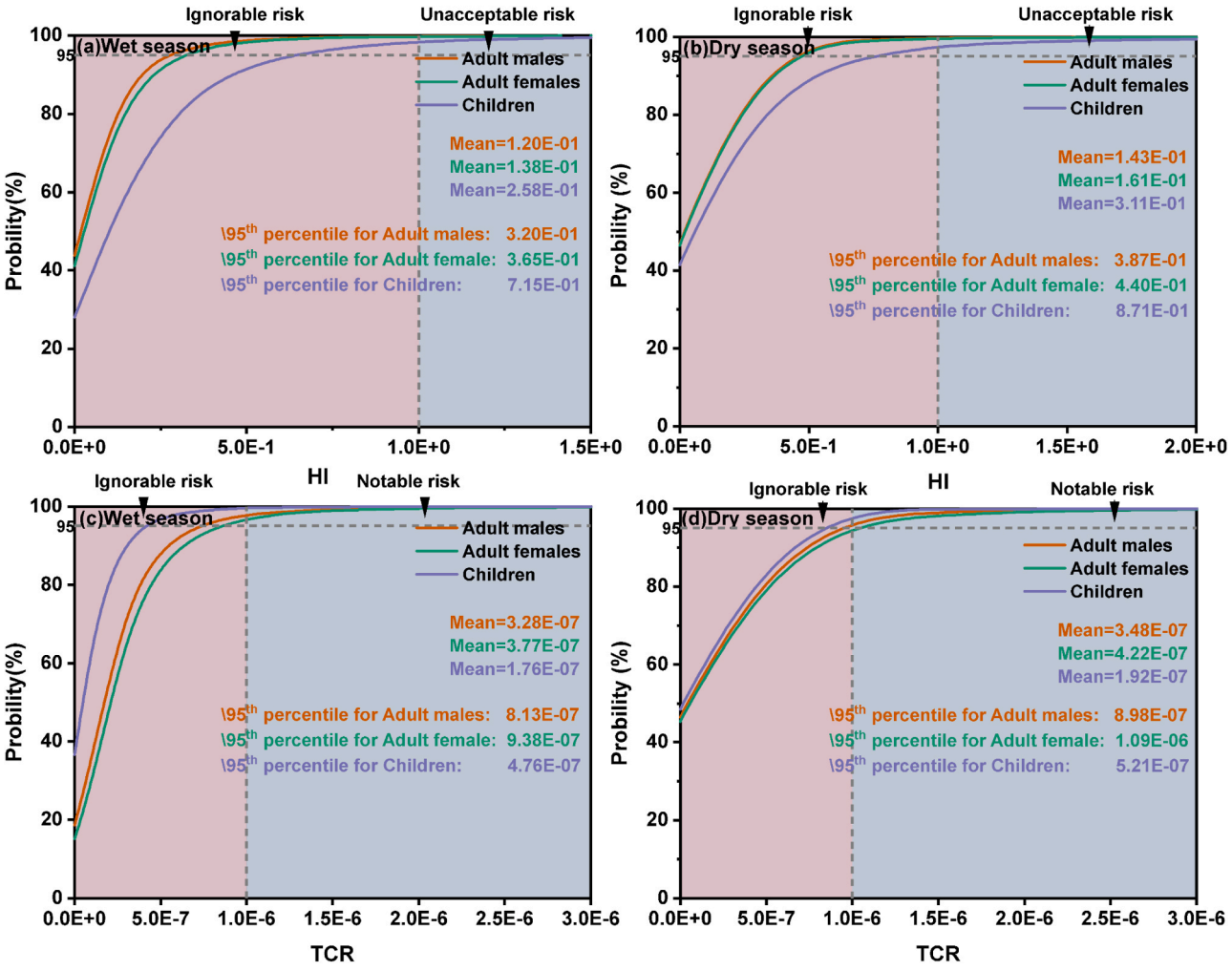

Fig. 4. Probability distribution of health risks in different populations during wet and dry seasons. (a) Noncarcinogenic risk in the wet season, (b) noncarcinogenic risk in the dry season, (c) carcinogenic risk in the wet season, and (d) carcinogenic risk in the dry season.

with a 95% probability. This suggests that the HI risk is negligible for all people, and no significant health risk is associated with exposure to the analyzed HMs. For the carcinogenic risk assessment, the mean TCR values were calculated for children, adult females, and adult males during the wet and dry water periods. During the wet period, the mean TCR values were 1.76E-07, 3.77E-07, and 3.28E-07 for children, adult females, and adult males, respectively. The 95% TCR values for all three populations were below the threshold of 1.0E-06, indicating that the calculated TCR values are within the safe range. However, the mean TCR values were 1.92E-07, 4.22E-07, and 3.48E-07 for children, adult females, and adult males, respectively, during the dry season. At the 95% confidence level, the total carcinogenic risk for children and adult males was below the threshold of 1.0E-06 and was within the safe range, but the total carcinogenic risk for adult females was above 1.0E-06 and requires attention.

The spatial distribution of HI in the three populations was similar, with HI in the central part of the study area being higher than that in the dry season, and the opposite was true in the northern part of the study area, with HI in the northern part of the study area being at a high value in both seasons (Fig. S2). The spatial distribution of TCR in the three populations was consistent, and the TCR showed the same seasonal pattern of change as HQ. The TCR value of point Y43 exceeded 1.0E-06 in both seasons, and there was a certain risk of carcinogenicity (Fig. S3).

3.3.2. Source-oriented health risk assessment

The findings suggest that particular attention should be given to controlling arsenic (As) levels in groundwater within the study area. During wet periods, priority should be placed on regulating industrial activities, while during dry periods, the focus should be on managing agricultural activities as the primary contributing source of pollution. For HI risk assessment, the HI values for all three sources (adult males, adult females, and children) were found to be below 1 during both the wet and dry water periods, indicating that the HI risk to the population was negligible. However, it should be noted that the contribution of pollution sources to the noncancer risk for different population groups during both periods was still significant. During the wet water period, the order of all three pollution sources to the noncarcinogenic risk, as well as the analyzed risk of carcinogenicity for both adults and children, was as follows: industrial (Factor II) > natural (Factor III) > agricultural (Factor I). This suggests that industrial activity posed the highest health risk to all three population groups in the wet period. In the dry period, the order of contribution to the noncancer risk for adults and children was as follows: agricultural activities (Factor II) > natural sources (Factor IV) > industrial activities (Factor III) > domestic sources (Factor I). Agricultural activities were identified as the largest source of noncancer risk for all three population groups during this period. Notably, the noncarcinogenic contribution of two elements, Cr and As, to all four factors was significantly higher than that of the others, both during the wet and dry water periods, with As contributing up to 84%. These findings highlight the importance of prioritizing these two elements in risk control, possibly due to the higher values of Reference Dose (RfD) for Cr and As. Previous studies have also established the potential carcinogenic risk of Cr and As (Long et al., 2021), consistent with the findings of this study.

3.3.3. Sensitivity analysis

The sensitivity analysis revealed that the concentrations of HMs in groundwater significantly impacted the health risk, with the intake rate (IR) playing a significant role (Tables S8-S9). Conversely, body weight (BW) and exposure frequency (EF) had a minor contribution of less than 10% to health risk, and BW showed a negative association with health risk. Regarding various groundwater HM sensitivity aspects in the study area, arsenic (As) was identified as the most substantial contributor to total noncarcinogenic and carcinogenic hazards. During periods of water abundance, As accounted for 67.70% of the total HI for adult males, 66.40% for adult females, and 52.30% for children (Table S10). Similarly, As contributed to 54.40% of the total carcinogenic risk for adult males, 53.80% for adult females, and 40.90% for children in the same period. However, during the dry period, the contribution of As increased to 70.70% for adult males, 70.00% for adult females, and 57.10% for children (Tables S9). It also accounted for 62.30% of the total TCR for adult males, 62.20% for adult females, and 47.80% for children.

3.4. Relationship between HMs, pollution sources, and health risks

The study results indicate that industrial and agricultural sources are the priority sources of HM pollution, requiring immediate control measures. Meanwhile, as mentioned above, we also need to focus on pollution control of the natural background and domestic emissions. Additionally, HMs have emerged as a priority element due to their significant contribution to health risks. Prior research has demonstrated that health risks are closely associated with the targeted HM toxicity coefficient and the wet metal content of pollution sources (R.J. Huang et al., 2018; J. Huang et al., 2018).

During the wet period, the contribution of different pollution sources to the carcinogenic risk showed significant variation. Agricultural activities, industrial activities, and natural sources contributed 2.97%, 74.10%, and 22.93%, respectively (Fig. 5 and Tables S12). Analysis of pollution sources revealed that agriculture accounted for 26.79%, primarily due to Cu (83.43%) and Zn (69.10%). However, their contribution to the carcinogenic risk was only 2.97%, mainly due to the relatively low carcinogenic coefficients of Cu and Zn. Industrial activities represented 50.68% of the total pollution sources, particularly with high levels of Pb (80.51%), As (91.89%), and Fe (94.75%). They contributed 74.10% to the carcinogenic risk, mainly due to the significant presence of As (91.89%) in industrial activities, leading to increased toxicity. Natural accounted for 22.53%, with Cr (49.16%) and Ni (94.75%) being the major components. Their contribution to the carcinogenic risk was 22.93%, which surpassed that of agricultural activities.

During the dry period, the contribution of different pollution sources to the carcinogenic risk varied significantly. Domestic sources, agricultural activities, industrial activities, and natural sources contributed 7.16%, 53.67%, 10.79%, and 28.37%, respectively, to the carcinogenic risk (Fig. 5 and Tables S9). Domestic sources accounted for 14.52%, primarily due to the presence of Fe (37.86%). Agricultural activities made up 25.38% of the total pollution sources, with As (63.36%) being the predominant pollutant. However, they contributed up to 53.84% of the carcinogenic risk, mainly due to the high load and toxicity of As in agricultural activities. Industrial activities accounted for 34.91%, especially with high levels of Ni (71.78%) and Pb (78.59%). Nevertheless, their contribution to the carcinogenic risk was only 10.83% due to the relatively low carcinogenic toxicity of Ni and Pb. Natural sources represented 25.19% of the total pollution sources, particularly with high levels of Cr (49.36%) and Zn (53.15%), which far exceeded levels from industrial activities. Natural sources contributed 28.46% to the carcinogenic risk. Cr and As were identified as the top two contributors to the TCR from various sources, indicating their potential carcinogenic risk, as concluded in previous studies..

This study identifies industrial and agricultural sources as priority control factors for groundwater pollution. To address these concerns, the following targeted pollution control recommendations are proposed: (1) Priority control of industrial and agricultural sources: Given the high demand for chemical fertilizers and pesticides in the study area, the government should promote the use of low-toxicity organic fertilizers to reduce reliance on chemical inputs in agriculture. Encouraging the development of modernized agriculture and urban tourism agriculture along major national highways and radial roads can lead to the integrated growth of urban and rural areas. Furthermore, establishing the Wuhan Airport Industrial Park can help develop industries such as new energy, jewelry and fashion, rail transportation, and vehicle

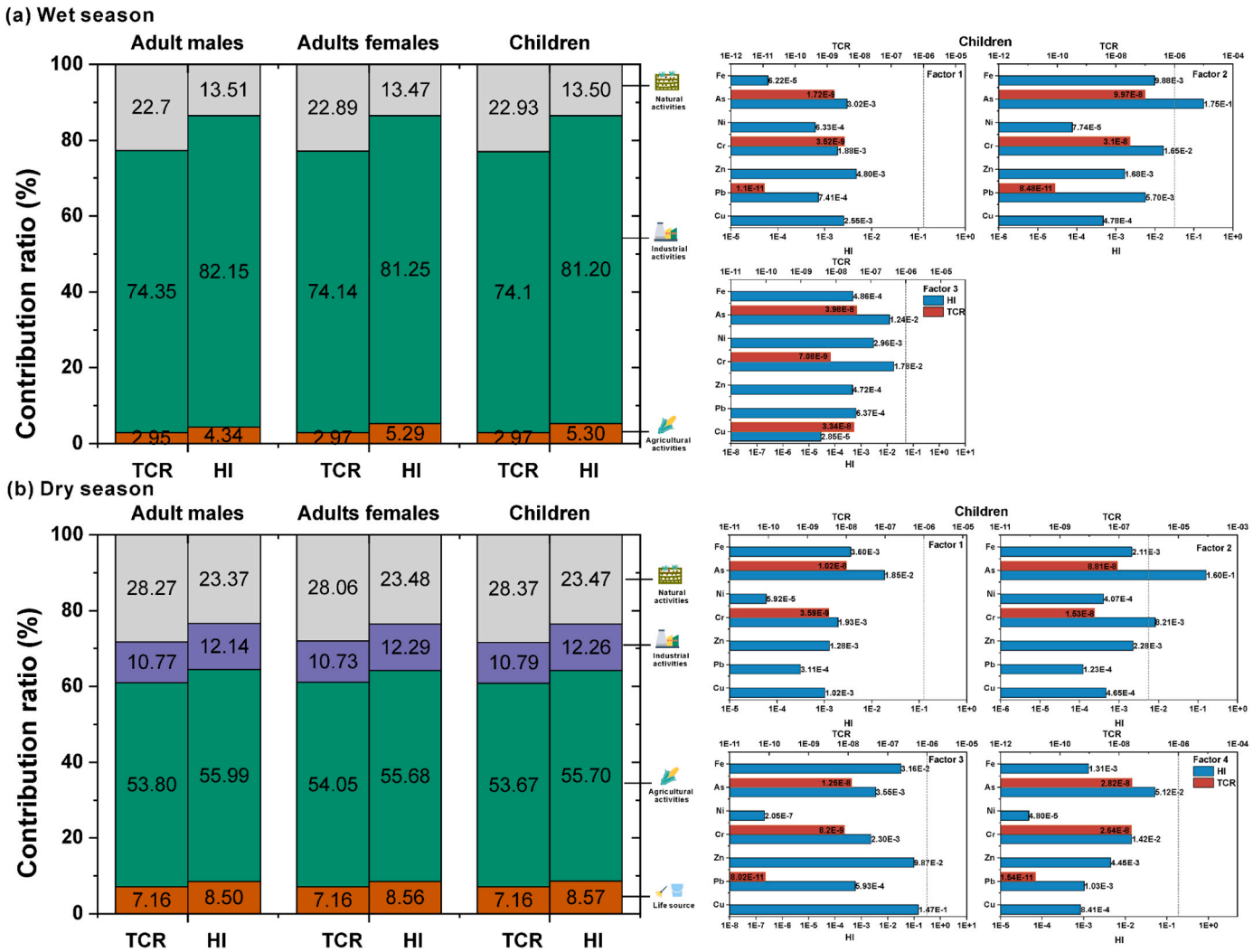

Fig. 5. Source-oriented map of HM's health risk contribution to groundwater during the (a) wet season and (b) dry season.

manufacturing, effectively reducing HM pollution from industrial waste. (2) Prioritize the Control of Arsenic (As) Pollution: Because pollution is a significant concern in the study area, mainly associated with industrial parks in the electronics, metal processing, and construction industries, a low-carbon transformation of traditional industries should be a focus of development in the Huangpi District. To reduce As emissions, efforts should be made to promote environmentally friendly technologies and practices. Implementing effective water treatment measures can significantly reduce HM contamination in the water supply.

4. Conclusions

The APCS/MLR and HRA models were used to quantify the relationship between HM concentrations, pollution sources, and health risks during wet and dry periods in groundwater in Huangpi District, Wuhan City, China, to prioritize control factors. The findings revealed that the sources of HMs in the groundwater varied between the dry and wet periods. The noncarcinogenic risk of HM pollutants to the population is acceptable, whereas the carcinogenic risk needs attention. Industrial and agricultural activities, as well as As, were identified as priority control factors for groundwater HM pollution. Our study provides valuable insights for the government and policymakers to prioritize pollution control measures and develop effective water quality management policies for groundwater. By understanding the pollution sources and elements that pose the greatest risks, targeted control policies can be formulated to reduce the management costs associated with groundwater pollution.

However, this study does have some limitations. The findings are specific to the Huangpi district of China. It may not be directly applicable to other areas with different geological, hydrogeological, and anthropogenic characteristics. Additionally, each method used in the assessment framework involves assumptions and simplifications. These assumptions could introduce uncertainties and potential biases in the results. Therefore, future studies on HM contamination in regions with high background values are warranted. We also need to analyze the heavy metal pollution of local domestic wastewater. Meanwhile, we should consider adding more constraints and uncertainty factors (such as changes in land use, industrial activities and geological features) to the model calculations and establishing direct links between priority control factors and specific human activities to enhance the models' accuracy.

CRediT authorship contribution statement

Wenjing Han and Yujie Pan: Methodology, Formal analysis, Investigation, Writing - original draft. **Emily Welsch, Xiaorui Liu and Shasha Xu:** Methodology, Supervision, Formal analysis, Writing review & editing. **Hongxia Peng and Changsheng Huang:** Investigation, Supervision and Data curation. **Jiarui Liu, Fangtin Wang, Xuan Li and Huanhuan Shi:** Conceptualization, Formal analysis, Software, Writing -

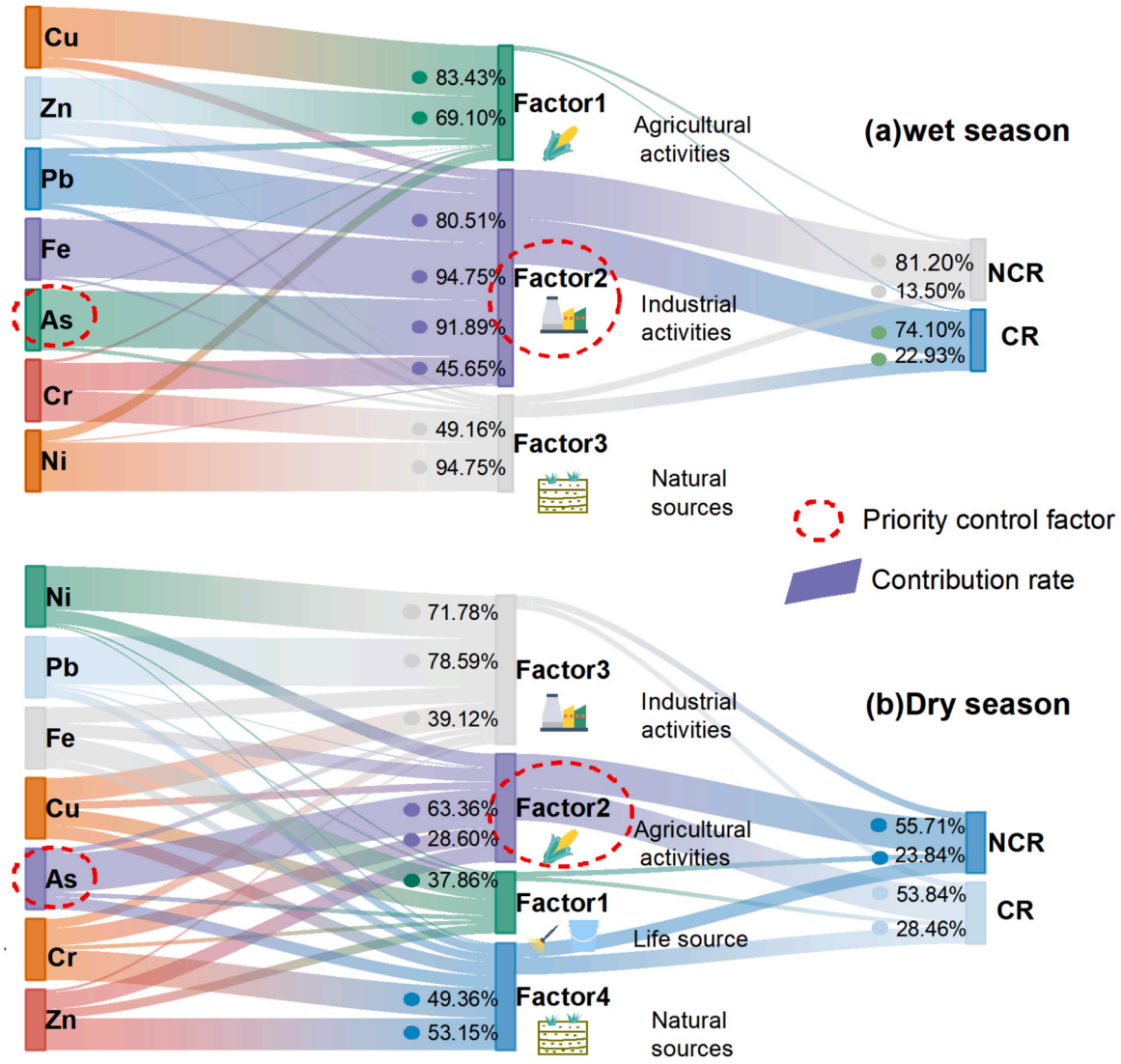

Fig. 6. The relationship between HMs, pollution sources, and health risks for the children: (a) the relationship in the wet season and (b) the relationship in the dry season.

review & editing. **Wei Chen:** Formal analysis.

Declaration of Competing Interest

The authors declare that they have no known competing financial interests or personal relationships that could have appeared to influence the work reported in this paper.

Data Availability

Data will be made available on request.

Acknowledgments

This work is supported by the National Natural Science Foundation of China (41877297) and the China Geological Survey (DD20190824, DD20190282).

Appendix A. Supporting information

Supplementary data associated with this article can be found in the online version at doi:10.1016/j.ecoenv.2023.115642.

References

Adeyemi, A.A., Ojekunle, Z.O., 2021. Concentrations and health risk assessment of industrial heavy metals pollution in groundwater in Ogun state, Nigeria. Scientific African 11 (1), 666.

Brtnický, M., Pecina, V., Hladký, J., Radziemska, M., Koudelková, Z., Klimánek, M., Richtera, L., Adamcová, D., Elbl, V., Galiová, M.V., Baláková, L., Kynický, J., Smolíková, V., Houška, J., Vaverková, M.D., 2019. Assessment of phytotoxicity, environmental and health risks of historical urban park soils. Chemosphere 220, 678–686.

Chorol, L., Gupta, S.K., 2023. Evaluation of groundwater heavy metal pollution index through analytical hierarchy process and its health risk assessment via Monte Carlo simulation. Process Saf. Environ. Prot. 170, 855–864.

Dehghani, F., Omidi, F., Fallahzadeh, R.A., Pourhassan, B., 2021. Health risk assessment of occupational exposure to heavy metals in a steel casting unit of a steelmaking plant using Monte–Carlo simulation technique. Toxicol. Ind. Health 37 (7), 431–440.

Dong, B., Zhang, R., Gan, Y., Cai, L., Freidenreich, A., Wang, K., Guo, T., Wang, H., 2019. Multiple methods for the identification of heavy metal sources in cropland soils from a resource-based region. Sci. Total Environ. 651, 3127–3138.

Feng, H., Wei, J., Cheng, Q., Gao, S., 2016. Spatial analysis of heavy metals contamination of shallow groundwater in relation to urban sprawl and intensive. Territ. Nat. Resour. Study 83–88.

Gao, J., Yuejun, Yang., 2009. Evaluation on ecological security in shiyanghe valley, gansu. Forest Resources Management.

Ginsberg, G.L., Belleggia, G., 2017. Use of Monte Carlo analysis in a risk-based prioritization of toxic constituents in house dust. Environ. Int. 109, 101–113.

Gu, Y.G., Lin, Q., Gao, Y.P., 2016. Metals in exposed-lawn soils from 18 urban parks and its human health implications in southern China's largest city, Guangzhou. Journal of Cleaner Production 115, 122–129.

Guo, C.Y., Wang, S.P., Chen, G., Hong, J., Huang, X., Lei, D.U., et al., 2017. Analysis and assessment on heavy metal contents of vegetable plantation soils in New Urban District of Wuhan. Hubei Agricultural Sciences 56, 43–46.
Guo, G., Wang, Y., Zhang, D., Li, K., Lei, M., 2023. Human health risk apportionment from potential sources of heavy metals in agricultural soils and associated uncertainty analysis. Environ. Geochem. Health 45 (3), 881–897.
He, J., Peng, K., Zeng, M.,. Environmental characteristics of high Fe and Mn groundwater in shallow aquifers at northeastern Jianghan Plai., 2016. South China Geology (03),258–264.
Herath, I.K., Wu, S., Ma, M., Ping, H., 2022. Heavy metal toxicity, ecological risk assessment, and pollution sources in a hydropower reservoir. Environ. Sci. Pollut. Res. 29 (22), 32929–32946.
Horton, R.K., 1965. An index number system for rating water quality. J. Water Pollut. Control Fed. 37 (3), 300–306.
Huang, C., Zhou, Y., Zhang, S., Wang, J., Liu, F., Gong, C., Yi, C., Li, L., Zhou, H., Wei, L., Pan, X., D., Shao, C., Li, Y., Han, W., Yin, Z., Li, X., 2021. Groundwater resources in the Yangtze River Basin and its current development and utilization. Geol. China 04, 979–1000.
Huang, J., Wu, Y., Sun, J., Li, X., Geng, X., Zhao, M., Sun, T., Fan, Z., 2021. Health risk assessment of heavy metal (loid) s in park soils of the largest megacity in China by using Monte Carlo simulation coupled with Positive matrix factorization model. J. Hazard. Mater. 415, 125629.
Huang, J., Guo, S., Zeng, G.M., Li, F., Gu, Y., Shi, Y., Shi, L., Liu, W., Peng, S., 2018. A new exploration of health risk assessment quantification from sources of soil heavy metals under different land use. Environ. Pollut. 243, 49–58.
Huang, R.J., Cheng, R., Jing, M., Yang, L., Li, Y., Chen, Q., Chen, Y., Yan, J., Lin, Chun, Zhang, R., Haddad, I., Prevot, A., Dowd, C., Cao, J., 2018. Source-specific health risk analysis on particulate trace elements: coal combustion and traffic emission as major contributors in wintertime Beijing. Environ. Sci. Technol. 52 (19), 10967–10974.
Jiang, C., Zhao, Q., Zheng, L., Chen, X., Li, C., Ren, M., 2021. Distribution, source and health risk assessment based on the Monte Carlo method of heavy metals in shallow groundwater in an area affected by mining activities, China. Ecotoxicol. Environ. Saf. 224, 112679.
Jiang, W., Liu, H., Sheng, Y., Ma, Z., Zhang, J., Liu, F., Chem, S., Meng, Q., Bai, Y., 2022. Distribution, source apportionment, and health risk assessment of heavy metals in groundwater in a multi-mineral resource area, North China. Expo. Health 14 (4), 807–827.
Jin, G., Fang, W., Shafi, M., Wu, D., Li, Y., Zhong, B., Ma, J., Liu, D., 2019. Source apportionment of heavy metals in farmland soil with application of APCS-MLR model: A pilot study for restoration of farmland in Shaoxing City Zhejiang, China. Ecotoxicol. Environ. Saf. 184, 109495.
Karami, M.A., Fakhri, Y., Rezania, S., Alinejad, A.A., Mohammadi, A.A., Yousefi, M., Ghaderpoori, M., Saghi, M.H., Ahmadpour, M., 2019. Non-carcinogenic health risk assessment due to fluoride exposure from tea consumption in Iran using Monte Carlo simulation. Int. J. Environ. Res. Public Health 16 (21), 4261.
Leung, C.M., Jiao, J.J., 2006. Change of groundwater chemistry from 1896 to present in the Mid-Levels area, Hong Kong. Environmental Geology 49, 946–959.
Li, P., Wu, T., Jiang, G., Pu, L., Wang, X., Zhang, J., Xu, F., Xie, X., 2022. Source identification and spatial differentiation of health risks of cultivated soil heavy metals in Jinhua City. Acta Scientiae Circumstantiae 42 (11), 10.
Liu, B., Cui, X., Wang, X., Hu, Q., 2023. Source identification and health risk assessment of heavy metals in groundwater of Yongqing County, Hebei Province. J. Ecol. Rural Environ. 39, 741–749.
Liu, J., Liu, Y.J., Liu, Y., Liu, Z., Zhang, A.N., 2018. Quantitative contributions of the major sources of heavy metals in soils to ecosystem and human health risks: A case study of Yulin, China. Ecotoxicol. Environ. Saf. 164, 261–269.
Liu, X., Zhang, L., 2017. Concentration, risk assessment, and source identification of heavy metals in surface sediments in Yinghai: a shellfish cultivation zone in Jiaozhou Bay, China. Mar. Pollut. Bull. 121 (1–2), 216–221.
Long, X., Liu, F., Zhou, X., Pi, J., Yin, W., Li, F., Huang, S., Ma, F., 2021. Estimation of spatial distribution and health risk by arsenic and heavy metals in shallow groundwater around Dongting Lake plain using GIS mapping. Chemosphere 269, 128698.
Lv, J., 2019. Multivariate receptor models and robust geostatistics to estimate source apportionment of heavy metals in soils. Environmental pollution 244, 72–83.
Ma, C., Zhou, J., Zeng, Y., Bai, F., Yan, Z., 2023. Source analysis and health risk assessment of heavy metals in groundwater in the Oasis Belt of Ruoqiang County, Xinjian. Acta Scientiae Circumstantiae, 43: 266–277.
Ma, W., Tai, L., Qiao, Z., Zhong, L., Wang, Z., Fu, K., Chen, G., 2018. Contamination source apportionment and health risk assessment of heavy metals in soil around municipal solid waste incinerator: a case study in North China. Sci. Total Environ. 631, 348–357.
Mahapatra, S.R., Venugopal, T., Shanmugasundaram, A., Giridharan, L., Jayaprakash, M., 2020. Heavy metal index and geographical information system (GIS) approach to study heavy metal contamination: a case study of north Chennai groundwater. Appl. Water Sci. 10, 1–17.
Masuda, H., 2018. Arsenic cycling in the Earth's crust and hydrosphere: interaction between naturally occurring arsenic and human activities. Progress in Earth and Planetary Science 5 (1), 1–11.
Mohan, S.V., Nithila, P., Reddy, S.J., 1996. Estimation of heavy metals in drinking water and development of heavy metal pollution index. J. Environ. Sci. Health Part A 31 (2), 283–289.
Muhammad, N., Lao, L., Intisar, A., Cui, H., Zhu, Y., 2019. Simultaneous determination of fluoride and chloride in iron ore by steam distillation followed by ion chromatography. Chromatographia 82 (12), 1839–1844.
Muhammad, N., Wang, F., Subhani, Q., Zhao, Q., Qadir, M.A., Cui, H., Zhu, Y., 2018. Comprehensive two-dimensional ion chromatography (2D-IC) coupled to a post-column photochemical fluorescence detection system for determination of neonicotinoids (imidacloprid and clothianidin) in food samples. RSC Adv. 8 (17), 9277–9286.
Muhammad, N., Zhang, Y., Subhani, Q., Intisar, A., Mingli, Y., Cui, H., Zhu, Y., 2020a. Comparative steam distillation based digestion of complex inorganic copper concentrates samples followed by ion chromatographic determination of halogens. Microchem. J. 158, 105176.
Muhammad, N., Ali, A., Hussain, I., Subhani, Q., Guo, D., Cui, H., Zhu, Y., 2023. Determination of fluorine and chlorine in standard steel residues and zinc sulfide concentrates by ion chromatography-Matrix interference study. Chin. J. Anal. Chem. 51 (2), 100147.
Muhammad, N., Zhang, Y., Asif, M., Khan, M.F.S., Intisar, A., Mingli, Y., Subhani, Q., Cui, H., Zhu, Y., 2020b. Feasibility of pyrohydrolysis and extended-steam distillation method for the extraction of two halides from zinc and lead concentrate samples followed by ion chromatography analysis. Microchem. J. 159, 105593.
Muhammad, N., Zia-ul-Haq, M., Ali, A., Naeem, S., Intisar, A., Han, D., Cui, H., Zhu, Y., Zhong, J., Rahman, A., Wei, B., 2021. Ion chromatography coupled with fluorescence/UV detector: A comprehensive review of its applications in pesticides and pharmaceutical drug analysis. Arab. J. Chem. 14 (3), 102972.
Muhammad, N., Hussian, I., Ali, A., Hussain, T., Intisar, A., Haq, I.U., Subhani, Q., Hedar, M., Zhong, J., Asif, M., Guo, D., Cui, H., Zhu, Y., 2022. A comprehensive review of liquid chromatography hyphenated to post-column photoinduced fluorescence detection system for determination of analytes. Arab. J. Chem., 104091
Nasrabadi, T., 2015. An IndexApproach toMetallic Pollution in RiverWaters. International Journal of Environmental Research 9 (1), 385–394.
Nilkarnjanakul, W., Watchalayann, P., Chotpantarat, S., 2022. Spatial distribution and health risk assessment of As and Pb contamination in the groundwater of Rayong Province, Thailand. Environmental Research 204, 111838.
Nimick, D.A., Moore, J.N., Dalby, C.E., Savka, M.W., 1998. The fate of geothermal arsenic in the Madison and Missouri Rivers, Montana and Wyoming. Water Resources Research 34 (11), 3051–3067.
Pan, Y., Ding, L., Xie, S., Zeng, M., Zhang, J., Peng, H., 2021. Spatiotemporal simulation, early warning, and policy recommendations of the soil heavy metal environmental capacity of the agricultural land in a typical industrial city in China: Case of Zhongshan City. Journal of Cleaner Production 285, 124849.
Pan, Y., Peng, H., Hou, Q., Peng, K., Shi, H., Wang, S., Zhang, W., Zeng, M., Huang, C., Xu, L., Pi, P., 2023. Priority control factors for heavy metal groundwater contamination in peninsula regions based on source-oriented health risk assessment. Science of The Total Environment 894, 165062.
Panda, G., Pobi, K.K., Gangopadhyay, S., Gope, M., Rai, A.K., Nayek, S., 2021. Contamination level, source identification and health risk evaluation of potentially toxic elements (PTEs) in groundwater of an industrial city in eastern India. Environ. Geochem. Health 1–25.
Peng, H., Hou, Q., Zeng, M., Huang, C., Shi, H., Pi, P., Pan, Y., 2021. Hydrochemical characteristics and controlling factors of groundwater in the Leizhou Peninsula. Environ. Sci. 42, 5375.
Proshad, R., Kormoker, T., Al, M.A., Islam, M.S., Khadka, S., Idris, A.M., 2022. Receptor model-based source apportionment and ecological risk of metals in sediments of an urban river in Bangladesh. J. Hazard. Mater. 423, 127030.
Qiao, J.J., 2004. Application of improved entropy method in Henan sustainable development evaluation. Resour. Sci. 26 (1), 113–119.
Qu, M., Chen, J., Huang, B., Zhao, Y., 2021. Source apportionment of soil heavy metals using robust spatial receptor model with categorical land-use types and RGWR-corrected in-situ FPXRF data. Environ. Pollut. 270, 116220.
Rasool, A., Farooqi, A., Masood, S., Hussain, K., 2016. Arsenic in groundwater and its health risk assessment in drinking water of, 22. HERA, Mailsi, Punjab, Pakistan, pp. 187–202.
Ravindra, K., Mor, S., 2019. Distribution and health risk assessment of arsenic and selected heavy metals in Groundwater of Chandigarh, India. Environ. Pollut. 250, 820–830.
Shi, H., Zeng, M., Peng, H., Huang, C., Sun, H., Hou, Q., Pi, P., 2022. Health Risk Assessment of Heavy Metals in Groundwater of Hainan Island Using the Monte Carlo Simulation Coupled with the APCS/MLR Model. Int. J. Environ. Res. Public Health 19 (13), 7827.
Shil, S., Singh, U.K., 2019. Health risk assessment and spatial variations of dissolved heavy metals and metalloids in a tropical river basin system. Ecol. Indic. 106, 105455.
Singh, K.R., Dutta, R., Kalamdhad, A.S., Kumar, B., 2020. Review of existing heavy metal contamination indices and development of an entropy-based improved indexing approach. Environment, Development and Sustainability, 22, 7847–7864.
Singh, R., Venkatesh, A.S., Syed, T.H., Reddy, A.G.S., Kumar, M., Kurakalva, R.M., 2017. Assessment of potentially toxic trace elements contamination in groundwater resources of the coal mining area of the Korba Coalfield, Central India. Environ. Earth Sci. 76, 1–17.
Smedley, P.L., Kinniburgh, D.G., 2002. A review of the source, behaviour and distribution of arsenic in natural waters. Applied geochemistry 17 (5), 517–568.
Song, Y., Li, H., Li, J., Mao, C., Ji, J., Yuan, X., Li, T., Ayoko, G., Frost, R., Feng, Y., 2018. Multivariate linear regression model for source apportionment and health risk assessment of heavy metals from different environmental media. Ecotoxicol. Environ. Saf. 165, 555–563.
Subhani, Q., Muhammad, N., Huang, Z., Asif, M., Hussain, I., Zahid, M., Hairong, C., Zhu, Y., Guo, D., 2020. Simultaneous determination of acetamiprid and 6-chloro-nicotinic acid in environmental samples by using ion chromatography hyphenated to online photoinduced fluorescence detector. J. Sep. Sci. 43 (20), 3921–3930.

Sun, J., Zhao, M., Huang, J., Liu, Y., Wu, Y., Cai, B., Han, Z., Huang, H., Fan, Z., 2022. Determination of priority control factors for the management of soil trace metal (loid) s based on source-oriented health risk assessment. J. Hazard. Mater. 423, 127116.

Sun, J., Huang, X., Song, X., Tang, R., Zhao, M., Cai, B., Wang, H., Han, Z., Liu, Y., Fan, Z., 2023. New insights into health risk assessment on soil trace metal (loid) s: Model improvement and parameter optimization. Journal of Hazardous Materials 458, 131919.

Tong, R., Yang, X., Su, H., Pan, Y., Zhang, Q., Wang, J., Long, M., 2018. Levels, sources and probabilistic health risks of polycyclic aromatic hydrocarbons in the agricultural soils from sites neighboring suburban industries in Shanghai. Sci. Total Environ. 616, 1365–1373.

Varol, M., 2019. Arsenic and trace metals in a large reservoir: seasonal and spatial variations, source identification and risk assessment for both residential and recreational users. Chemosphere 228, 1–8.

Varol, M., Tokatlı, C., 2022. Seasonal variations of toxic metal (loid) s in groundwater collected from an intensive agricultural area in northwestern Turkey and associated health risk assessment. Environ. Res. 204, 111922.

Wang, J., Li, S., Cui, X., Li, H., Qian, X., Wang, C., Sun, Y., 2016. Bioaccessibility, sources and health risk assessment of trace metals in urban park dust in Nanjing, Southeast China. Ecotoxicol. Environ. Saf. 128, 161–170.

Welch, A.H., Westjohn, D.B., Helsel, D.R., Wanty, R.B., 2000. Arsenic in ground water of the United States: Occurrence and geochemistry. Ground Water 38 (4), 589.

WHBS, 2018. Wuhan Statistical Yearbook. Wuhan Bureau of Statistics.

WHBS, 2019. Wuhan Statistical Yearbook. Wuhan Bureau of Statistics.

WHBS, 2020. Wuhan Statistical Yearbook. Wuhan Bureau of Statistics.

Wu, J., Bian, J., Wan, H., Sun, X., Li, Y., 2021. Probabilistic human health-risk assessment and influencing factors of aromatic hydrocarbon in groundwater near urban industrial complexes in Northeast China. Sci. Total Environ. 800, 149484.

Wu, Z., Chen, Y., Han, Y., Ke, T., Liu, Y., 2020. Identifying the influencing factors controlling the spatial variation of heavy metals in suburban soil using spatial regression models. Sci. Total Environ. 717, 137212.

Yang, S., Zhao, J., Chang, S.X., Collins, C., Xu, J., Liu, X., 2019. Status assessment and probabilistic health risk modeling of metals accumulation in agriculture soils across China: A synthesis. Environ. Int. 128, 165–174.

Yang, Y., Christakos, G., Guo, M., Xiao, L., Huang, W., 2017. Space-time quantitative source apportionment of soil heavy metal concentration increments. Environ. Pollut. 223, 560–566.

Yu, Z., Hu, X., Liu, W., Chen, W., Ke, Y., 2014. Pollution characteristics and health risk assessment of heavy metals in suburban agricultural areas of Wuhan, China. Res. Environ. Sci. 27, 881–887.

Yuan, B., Cao, H., Du, P., Ren, J., Chen, J., Zhang, H., Zhang, Y., Luo, H., 2023. Source-oriented probabilistic health risk assessment of soil potentially toxic elements in a typical mining city. J. Hazard. Mater. 443, 130222.

Zhai, Y., Zheng, F., Li, D., Cao, X., Teng, Y., 2022. Distribution, genesis, and human health risks of groundwater heavy metals impacted by the typical setting of songnen plain of NE China. Int. J. Environ. Res. Public Health 19 (6), 3571.

Zhang, M., Wang, X., Liu, C., Lu, J., Qin, Y., Mo, Y., Xiao, P., Liu, Y., 2020. Quantitative source identification and apportionment of heavy metals under two different land use types: comparison of two receptor models APCS-MLR and PMF. Environ. Sci. Pollut. Res. 27, 42996–43010.

Zhang, W.H., Yan, Y., Yu, R.L., Hu, G.R., 2021. The sources-specific health risk assessment combined with APCS/MLR model for heavy metals in tea garden soils from south Fujian Province, China. Catena 203, 105306.

Zhang, Y., Hu, Y., Tao, L., Zhou, F., Yang, Q., Liu, L., 2021. Hydrochemical characteristic and formation mechanism in the Yangtze River Demonstration District, Wuhan City. Acta Sci. Circumstantiae 41 (3), 9.

Zhou, J., Jiang, Z., Xu, G., Qin, X., Huang, Q., Zhang, K., 2019. Distribution and health risk assessment of metals in groundwater around iron mine. China Environ. Sci. 39, 11.